Supplemental materials for:

Molecular Weight and Uniformity Define the Mechanical Performance of Lignin-based Carbon Fiber

Qiang Li[1,2,3], Wilson K. Serem[4], Wei Dai[5], Yuan Yue[5,6], Mandar T. Naik[7], Shangxian Xie[1,2,3], Pravat Karki[8], Li Liu[6,9], Hung-Jue Sue[10], Hong Liang[5], Fujie Zhou[7], Joshua S. Yuan[1,2,3*]

[1]Synthetic and Systems Biology Innovation Hub, Texas A&M University, College Station, TX 77843, USA

[2]Department of Plant Pathology and Microbiology, Texas A&M University, College Station, TX 77843, USA

[3]Institute for Plant Genomics and Biotechnology, Texas A&M University, College Station, TX 77843, USA

[4]Material Characterization Facility, Texas A&M University, College Station, TX 77843, USA

[5]Department of Mechanical Engineering, Texas A&M University, College Station, TX 77843, USA

[6]Department of Materials Science and Engineering, Texas A&M University, College Station, TX 77843, USA

[7]Biomolecular NMR Laboratory, Department of Biochemistry and Biophysics, Texas A&M University, College Station, Texas 77843, USA

[8]Texas A&M Transportation Institute, Texas A&M University, College Station, TX 77843, USA

[9]Department of Chemistry, Texas A&M University, College Station, TX 77843, USA

[10]Polymer Technology Center, Department of Materials Science and Engineering, Texas A&M University, College Station, TX 77843, USA

*For correspondence: Joshua S. Yuan: syuan@tamu.edu

Materials

The industrial Kraft lignin (with low sulfonate content, catalog number: 370959) was purchased from Sigma–Aldrich (USA). Polyacrylonitrile (PAN) with molecular weight of 150,000 was obtained from Pfaltz & Bauer, USA. The enzyme (laccase from trametes versicolor, 0.5 U/mg, catalog number: 38429) and other chemicals and reagents used in this research are the products of Sigma–Aldrich (USA).

Enzymatic processing of Kraft lignin

The enzymatic processing of Kraft lignin was carried out according to our previous report with modifications.[1,2] Briefly, Kraft lignin was treated with laccase (15 mg/g lignin) and 1-hydroxy benzotriazolehydrate (HBT, 25 mg/g lignin) at a 10 wt% concentration for 48 h in a Biostat® A reactor (Sartorius, Bohemia, NY). The oxygen was supplied to lignin solution with a flow rate at 5 ccm. The temperature and the stirring speed were controlled at 50 °C and 200 rpm, respectively. After the treatment, the lignin sample was centrifuged to render water-insoluble and water-soluble fractions. The water-insoluble fraction was washed with 200 mL of iced deionized water for three times before centrifugation and lyophilization for dry lignin powders.

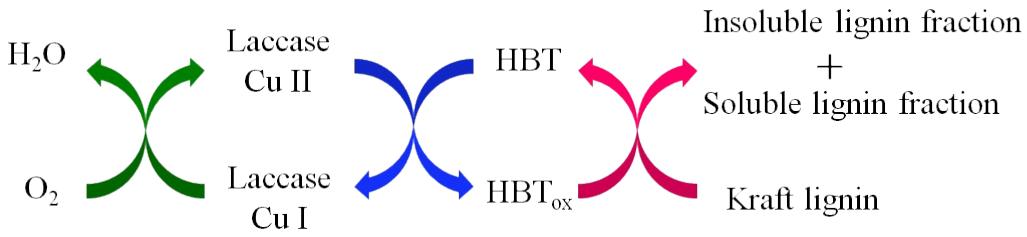

Fig. S1. Enzyme-mediator processing of industrial Kraft lignin derives water-insoluble and water-soluble lignin fractions.

As shown in Fig. S1, HBT served as the electron mediator in the system and could improve the fractionation of lignin by accelerating the electron transfer and facilitate the redox reaction penetration into macromolecule during the oxidation by laccase.[1,2] The water-soluble fraction was depolymerized lignin with approximately 30 w% of raw Kraft lignin, whilst water-insoluble fraction yielded about 70 w%.

Fractionation of lignin with dialysis

Five grams of the water-insoluble lignin fraction from the laccase/HBT processing was dissolved in 100 mL of 0.03 N aqueous NaOH solution. The lignin solution was then transferred into regenerated cellulose dialysis tubes (Fisher Scientific, USA) with 3 500 (3.5K), 6 000-8 000 (6K), and 12000-14000 (12K) nominal molecule weight cutoff, respectively. Lignin was dialyzed against 2 L of MilliQ water for one week with the exchange of fresh MilliQ water every day. The dialyzed was precipitated by adjusting its pH into 2 with 1 M hydrochloric acid solution. After 1 h stirring for completely precipitation, dialyzed lignin sample can be obtained by centrifugation (25 000 g) and lyophilization. The yields of lignin fractions processed by dialysis are 82.0 %, 73.0 %, and 64.6 % for 3.5K, 6K, and 12K cutoff dialysis tubes, respectively.

Gel Permeation Chromatography (GPC)

Before GPC characterization, all lignin samples were acetylated as described before[3] to obtain acetylated lignin. GPC analysis was performed using an OMNISEC system (Malvern Instrument Ltd., Houston, TX). Two D6000 and one T2000 Viscotek D-Columns (Malvern, Houston, TX) were connected in series. Column temperature was set at 45 ^{o}C. Tetrahydrofuran (THF) was used

as the eluent at a flow rate of 1.0 mL/min. RI detector, UV detector (280 nm), and a viscometer installed in the OMNISEC REVEAL system was used for monitoring fractions. The acetylated lignin was dissolved in THF with the concentration of 1 mg/mL, and 100 μL of the samples was injected into the GPC system after filtration with 0.45 μm membrane filter (VWR, Houston, TX). Universal calibration curve was established with polystyrenes as standards.

We observed a significant batch-to-batch difference of molecular weight for the lignin samples. Commercial lignin as a byproduct of pulping mills has unpredictable specifications since numerous process variations like cooking conditions could affect the final production of lignin.[4] Nevertheless, the increment in lignin molecular weight after laccase/HBT treatment was consistent for the same batch of lignin, suggesting the liability of our GPC measurement. The molecular weight (Mn) and PDI of water-insoluble and dialyzed lignin fractions were shown in Fig. 1B and 1C, respectively. The water-soluble lignin fraction in this research had the Mn of 3375 g/mol and PDI of 2.642, which were remarkably decreased as compared to the raw Kraft lignin.

Table S1. Mw (g/mol) of lignin fractions.

KL-Raw	KL-L/H-Insol.	KL-L/H-Insol.-3.5K	KL-L/H-Insol.-6K	KL-L/H-Insol.-12K	80% KL-12K+20% KL-Raw
38674	40911	45167	44519	55592	76560

Abbreviations of lignin fractions are in the caption of Figure 1.

Electrospinning

Lignin precursor fibers were produced via electrospinning (Fig. S2). Briefly, the grounded lignin and PAN powders were mixed at a ratio of 1:1 (w/w) and then dissolved in DMF to render a 15 w% solution. Lignin/PAN mixture was then loaded in a 10 mL syringe with a 22 gauge (i.d. 0.70 mm, length 38 mm) stainless steel blunt needle (Terumo, Yokohama, Japan). Electrospinning was carried out in a nanofiber electrospinning unit (Kato Tech Co., Ltd., Kyoto, Japan) at the followed

conditions: Solution feed rate, 0.25 mL/h; applied voltage, 9.5 kV; the distance between the syringe needle and the aluminum disc, 17 cm. The formed fiber mat was picked off from the aluminum foil and then kept in desiccator.

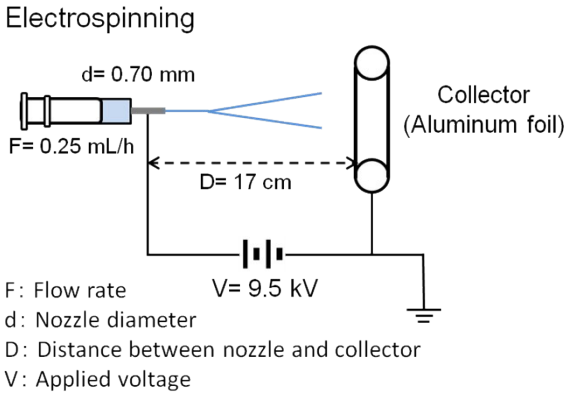

Fig S2. Schematic illustration of electrospinning.

Thermostabilization and carbonization

Both thermostabilization and carbonization of lignin precursor fibers were conducted in a split tube furnace with vacuum system (GSL 1600X, MTI Corporation, Richmond, CA). The heating processes for thermostabilization and carbonization were shown in Fig. S3A and S3B, respectively. Thermostabilization was carried out in air environment, whilst the carbonization was performed under N_2 atmosphere (240 cm^3/min) after exchanging the air in the tube furnace with nitrogen gas three times by purging with vacuum pump to 10^{-2} torr.

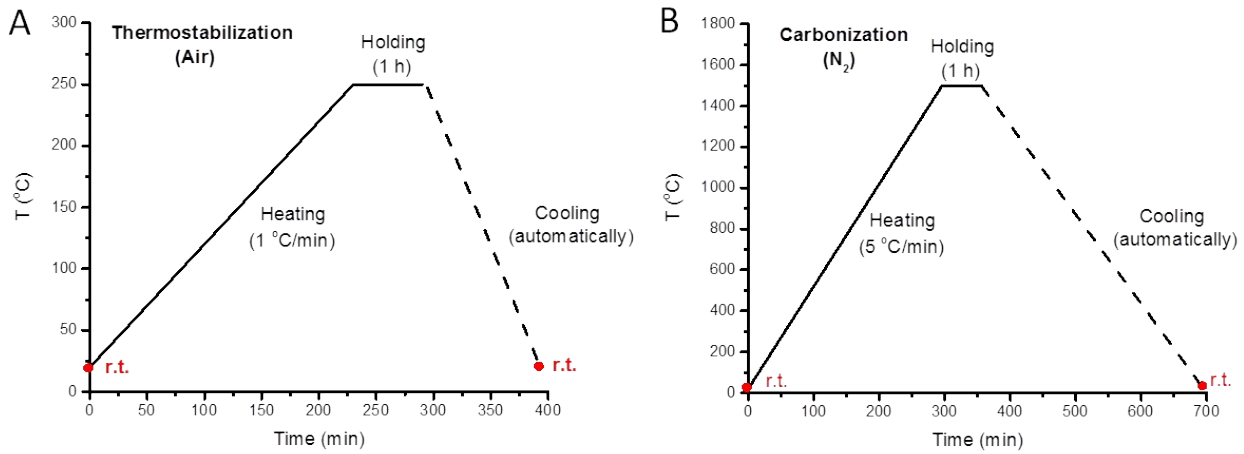

Fig. S3. Heating processes for thermostabilization (A) and carbonization (B).

Field emission scanning electron microscope (FE-SEM)

Images for the morphologies of carbon fibers were taken with a FEI Quanta 600F FE-SEM (FEI Company, Hillsboro, OR). The fibers were coated with Au/Pd (10 nm thickness) with a Cressington 208 HR sputter coater (TED PELLA INC., Redding, CA). The working distance was 10 mm, and the accelerating voltage was 5 kV. The diameters of carbon fibers were measured using ImageJ software (https://imagej.nih.gov/ij/). The reported diameters were the average data of at least 40 different carbon fibers. The morphologies of carbon fibers were displayed in both Fig. 2 and Fig. S4.

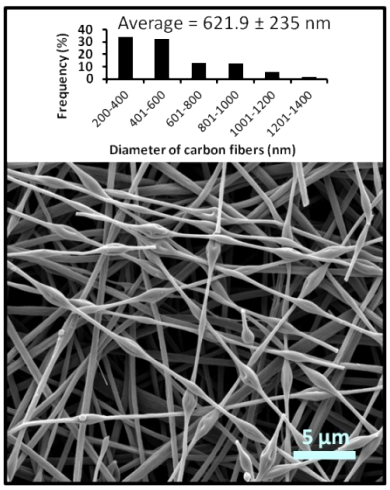

111

112 Fig. S4. SEM image of the carbon fiber made from the mixed lignin fraction (50 w% of KL-L/H-
113 Insol.-12K mixed with 50 w% of KL-Raw).

114 **Nanoindentation**

115 Elastic modulus and harness of carbon fibers were measured with Hysitron TI 950 Triboindenter
116 (Minneapolis, MN). Before the measurement, fibers were embedded in Epofix™ epoxy resins
117 (Electron Microscopy Science, Hatfield, PA), and then polished with a RMC Boeckeler
118 MTX microtome (Boeckeler Instruments Inc., Tucson, AZ) and a EcoMet 3 grinder/polisher
119 (Buehler, Lake Bluff, IL). The transverse sections of fibers were indented using a Cube Corner
120 (90°) tip with 40 nm radius. The calibration of the tip was performed on a fused quartz standard.
121 The indentation depth was set at 15-20 nm to avoid the effects of substrate (resin) on the
122 measurement.[5] Twenty-five indents were conducted on five different carbon fibers for each sample
123 selected under SPM imaging (Fig. S5A). The reduced elastic modulus (E_r) and the hardness (H)
124 were obtained using the following equations[6]:

$$E_r = \frac{\sqrt{\pi}}{2\sqrt{A}} \times S \quad (1)$$

125

$$H = \frac{P_{max}}{A} \tag{2}$$

where E_r is the reduced elastic modulus, A is the contact area, S is the stiffness which is calculated as the slope of initial unloading curve in loading-displacement (P-h) curve (Fig. S5B), H is the hardness, P_{max} is the applied maximum.

The hardness for all carbon fibers made from fractionated lignin did not show significant differences (Fig. S6). However, hardness was decreased when KL-Raw was added into KL-L/H-Insol.-12K (both 80% KL-12K+20% KL-Raw and 50% KL-12K+50% KL-Raw in Fig. S6). Small molecules may render the decreases in the hardness. The relationship between the reduced elastic modulus (E_r) and Young's modulus is shown in the equation (3). However, the Poisson's ratio of our carbon fiber (v_s) is unknown in this study, which makes the Young's modulus of our carbon fiber unknown.

$$\frac{1}{E_r} = \frac{(1 - v_i^2)}{E_i} + \frac{(1 - v_s^2)}{E_s} \tag{3}$$

Where E_i and E_s are the Young's modulus of indenter (1140 GPa) and sample respectively. v_i and v_s are the Poisson's ratio of indenter (0.07) and sample respectively.

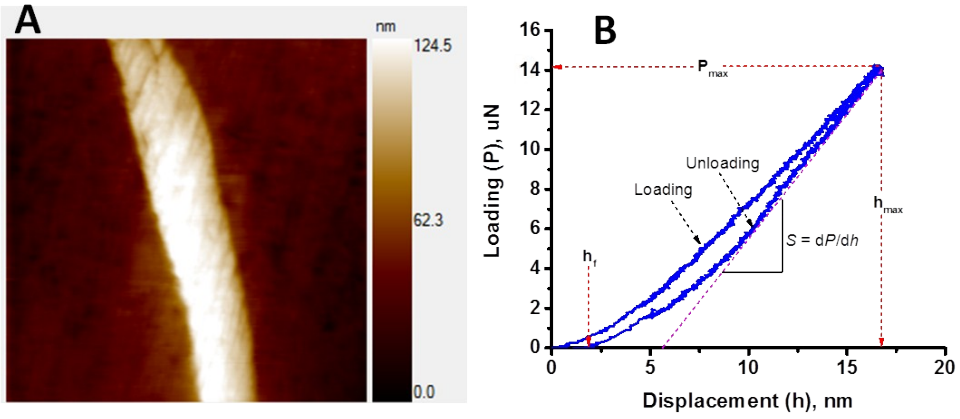

Fig S5. An example (KL-L/H-Insol.) of topography of scanning probe microscopy (SPM) under nanoindentation (A) and the loading-displacement curve (B). P_{max} is the maximum loading, h_{max} is the maximum displacement, h_f is the final displacement, S is the stiffness. Plotting this figure was referred to Oliver and Pharr 1992.[6]

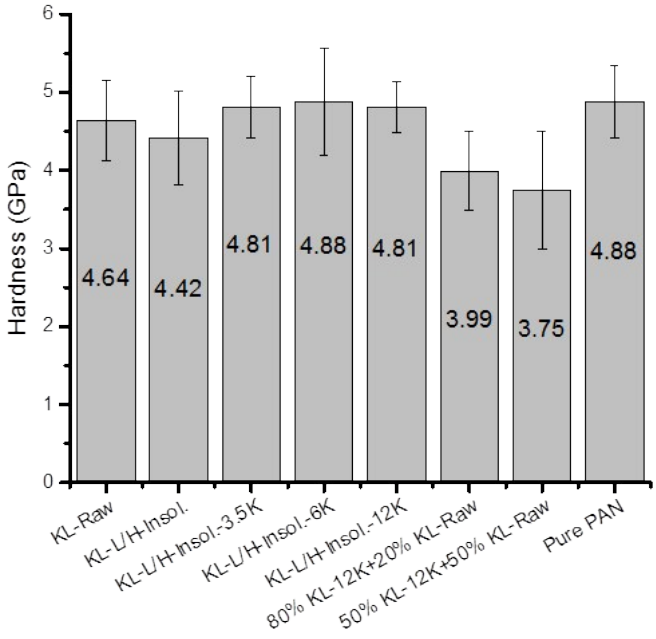

Fig. S6.The hardness of the carbon fibers.

Tensile strength of fiber mat

The tensile strength of carbon fiber mats were measured using a load cell configured on a stretching system. For the measurement, fiber mats were cut into pieces with about 3 mm in width and 12 mm in length, and then mounted on paper sheets with slots. The test was performed with the strain rate of 0.06/s and the acquisition rate of 100 Hz. Both force and displacement were recorded. To get a stress-strain curve, the area of fiber mat cross section was calculated as followed:

$$A_s = V_s / L_s,\ V_s = \rho_s / m_s$$

Where A_s is the area of sample cross section; V_s, L_s, ρ_s and m_s are the volume, length, density and weight of the sample, respectively. All measurements were repeated three times.

As shown in Fig. S7, tensile strengths of carbon fiber mats made from dialyzed lignin fractions (KL-L/H-Insol.-3.5K, KL-L/H-Insol.-6K, and KL-L/H-Insol.-12K) were higher than that of KL-Raw, suggesting that the removal of small lignin molecules could improve the tensile strength of fiber mats. Moreover, fiber mat made of more uniform lignin fractions (KL-L/H-Insol.-3.5K, KL-L/H-Insol.-6K, and KL-L/H-Insol.-12K) had higher tensile strength as compared to the less uniform fractions (KL-Raw, KL-L/H-Insol., and 80%KL-12K+20%KL-Raw). The results from tensile strength of fiber mats well corroborate the data from nanoindentation to indicate that lignin uniformity could improve the mechanical performance of lignin-based carbon fiber. In the future work, we will develop novel technologies to study the tensile strength of a single nanofiber to further define the impact of molecular weight and uniformity.

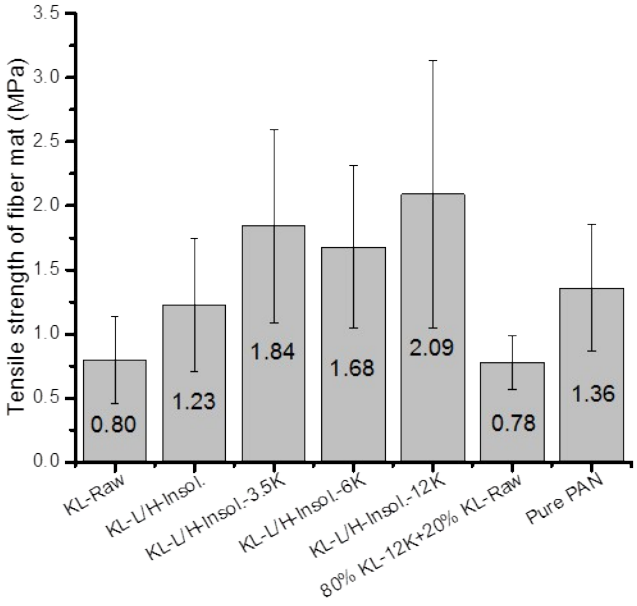

Fig. S7. Tensile strength of carbon fiber mats.

Thermogravimetric analysis (TGA) and differential scanning calorimetry (DSC)

Both TGA and DSC were performed on thermostabilized lignin precursor fibers. TGA measurement was conducted using TA Instruments Q600-SDT system (New Castle, DE) under N_2 atmosphere (100 mL/min) with the heating rate of 10 ^oC/min from room temperature to 1450 ^oC. DSC analysis was performed using TA Instrument DSC-Q2000 system with two heating cycles under a nitrogen atmosphere. Fibers were heated from room temperature to 350 ^oC at the heating rate of 20 ^oC/min and then cooled down to 0 ^oC with a rate of 20 ^oC/min. The second cycle was repeated at the same heating/cooling condition.

TGA and DTG curves were shown in Fig. S8, and the residue weights of fibers derived from the TGA curve were shown in the Table S2. The rapid weight losses for most fibers were found between 350-400 ^oC (Fig. S8A and S8B), which might be due to the reaction of the liable oxygen containing group.[7] The rapid weight losses for the fibers made of the mixed lignin (80 % KL-12K+20% KL-Raw) was between 400-600 ^oC. The final yields of lignin-based carbon fibers made of both KL-L/H-12K and the mixed fraction (80 % KL-12K+20% KL-Raw) at 1440 ^oC were lower than other carbon fibers (Table S2). This might induced by the high content of the oxygen containing group in the lignin fractions.[7]

Glass transmission temperature (T_g) could be derived from the second cycle of DSC analysis (Fig. S9). T_g indicates the miscibility of polymers in blend.[8] As shown in Fig. S9, both laccase/HBT treated lignin and dialyzed lignin had lower T_g than raw Kraft lignin, suggesting the fractionated lignin had better miscibility with the PAN polymer in lignin-PAN precursor fibers. The improved miscibility of the fractionated lignin could also benefit the spinnability for the fine precursor fibers.

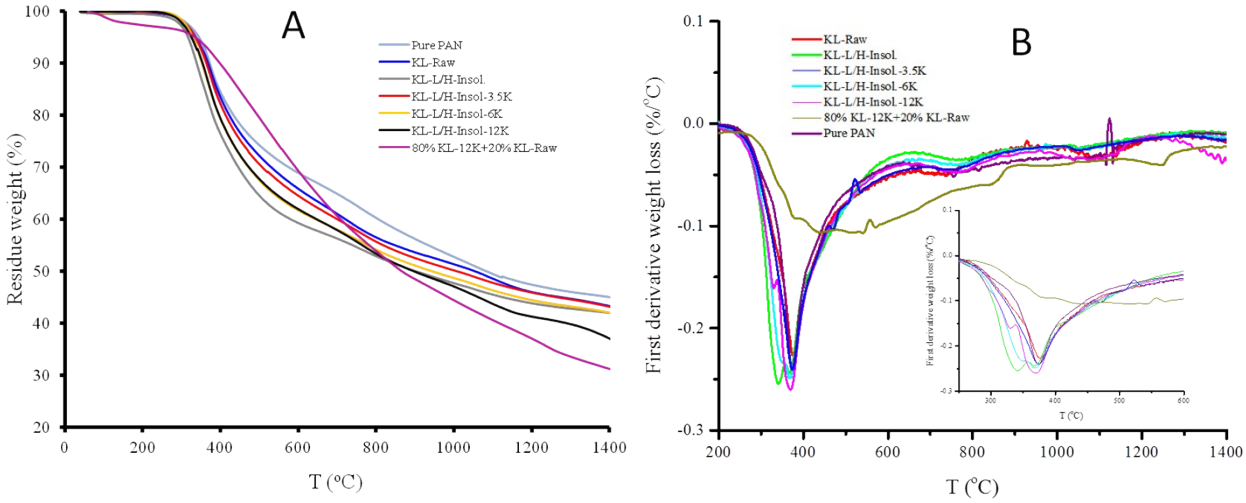

193

194 Fig. S8. TGA (A) and DTG (B) of thermostabilized carbon fiber precursors. The inserted figure in

195 B is the magnified DTG curve at 200-600 °C.

196

197 Table S2. Residue weight (%) of precursor fibers during carbonization derived from TGA curves.

	200 °C	350 °C	500 °C	650 °C	800 °C	1200 °C	1440 °C
Pure PAN	99.7	94.4	74.3	66.9	60.3	47.4	44.5
KL-Raw	99.8	93.2	72.2	63.4	56.5	46.0	42.2
KL-L/H-Insol.	99.4	87.3	64.6	57.8	53.0	43.9	41.7
KL-L/H-Insol.-3.5K	99.9	92.8	70.6	62.2	55.7	45.9	42.4
KL-L/H-Insol.-6K	100	90.4	67.5	59.8	54.2	44.5	41.4
KL-L/H-Insol.-12K	100	90.7	67.7	59.9	53.4	41.2	35.0
80% KL-12K+20% KL-Raw	98.9	94.1	79.5	64.7	53.9	37.1	30.1

198

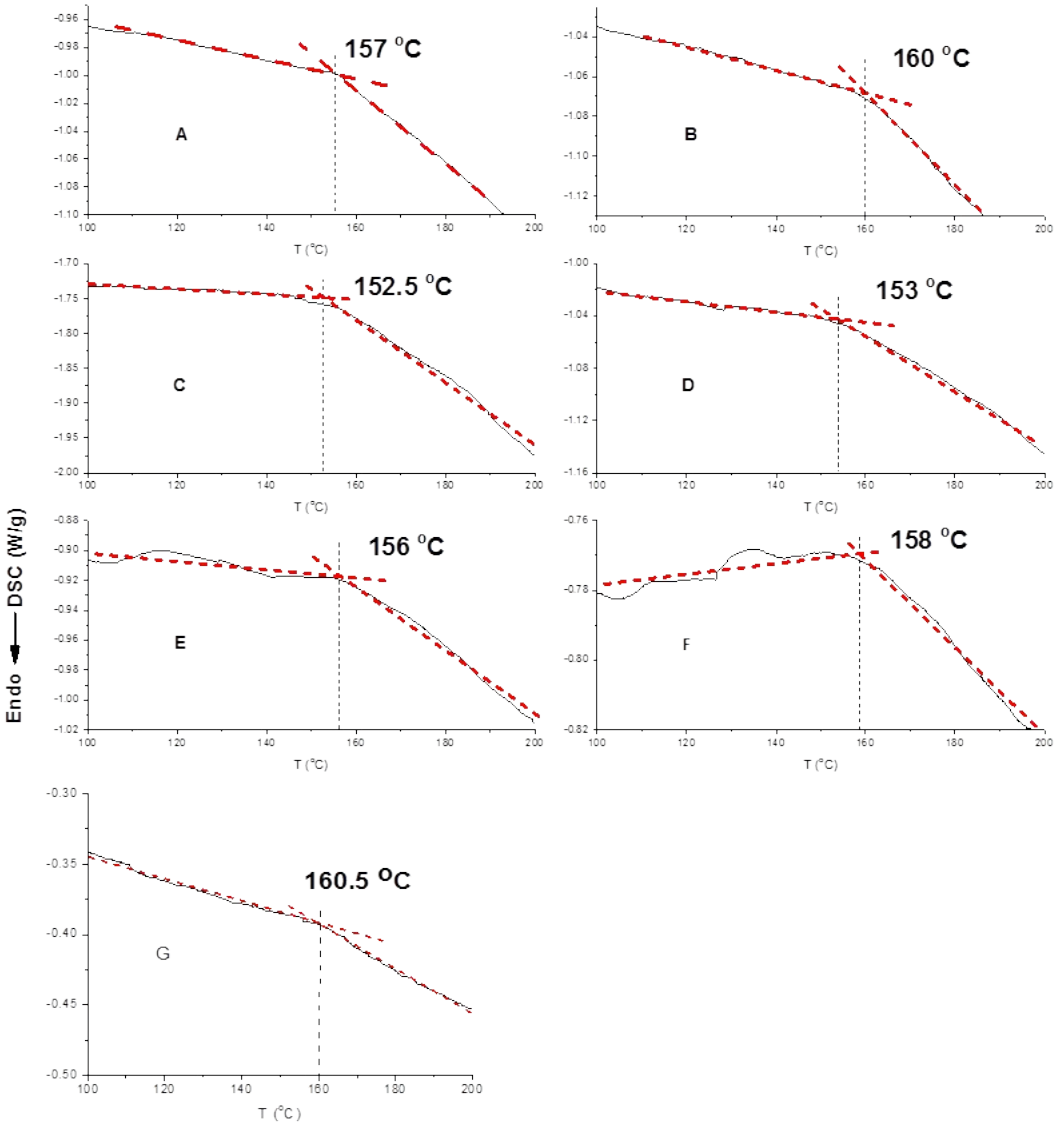

Fig. S9. Glass transmission temperature (T_g) of thermostabilized precursor fibers made of lignin/PAN composite and pure PAN. The heating flow curves were derived from the second heating cycle of DSC analysis. A, pure PAN; B, KL-Raw; C, KL-L/H-Insol.; D, KL-L/H-Insol.-3.5K; E, KL-L/H-Insol.-6K; F, KL-L/H-Insol.-12K; G, 80 % KL-12K+20 % KL-Raw.

Raman spectroscopy

G/D ratio of carbon fiber was analyzed with Raman spectroscopy. A piece of carbon fiber mat was cut and then fixed on a glass slide using double adhesive tapes. Raman spectra of carbon fibers

were recorded with a Horiba Jobin-Yvon LabRam Raman Cofocal Microscope system using 633 nm laser, 10× magnification of objective lens, D0.3 filter, 200 μm confocal pinhole, 10s exposure time, and 10 accumulations. The obtained Raman spectra were re-plotted and analyzed with Origin 9 software using Guassian curve fitting. As shown in Fig. S10, Raman shift of D band and G band are near 1348 $cm^{-1}$and 1581 cm^{-1}, respectively. Such Raman shifts of D and G bands were also confirmed with the commercial graphite (data not shown).

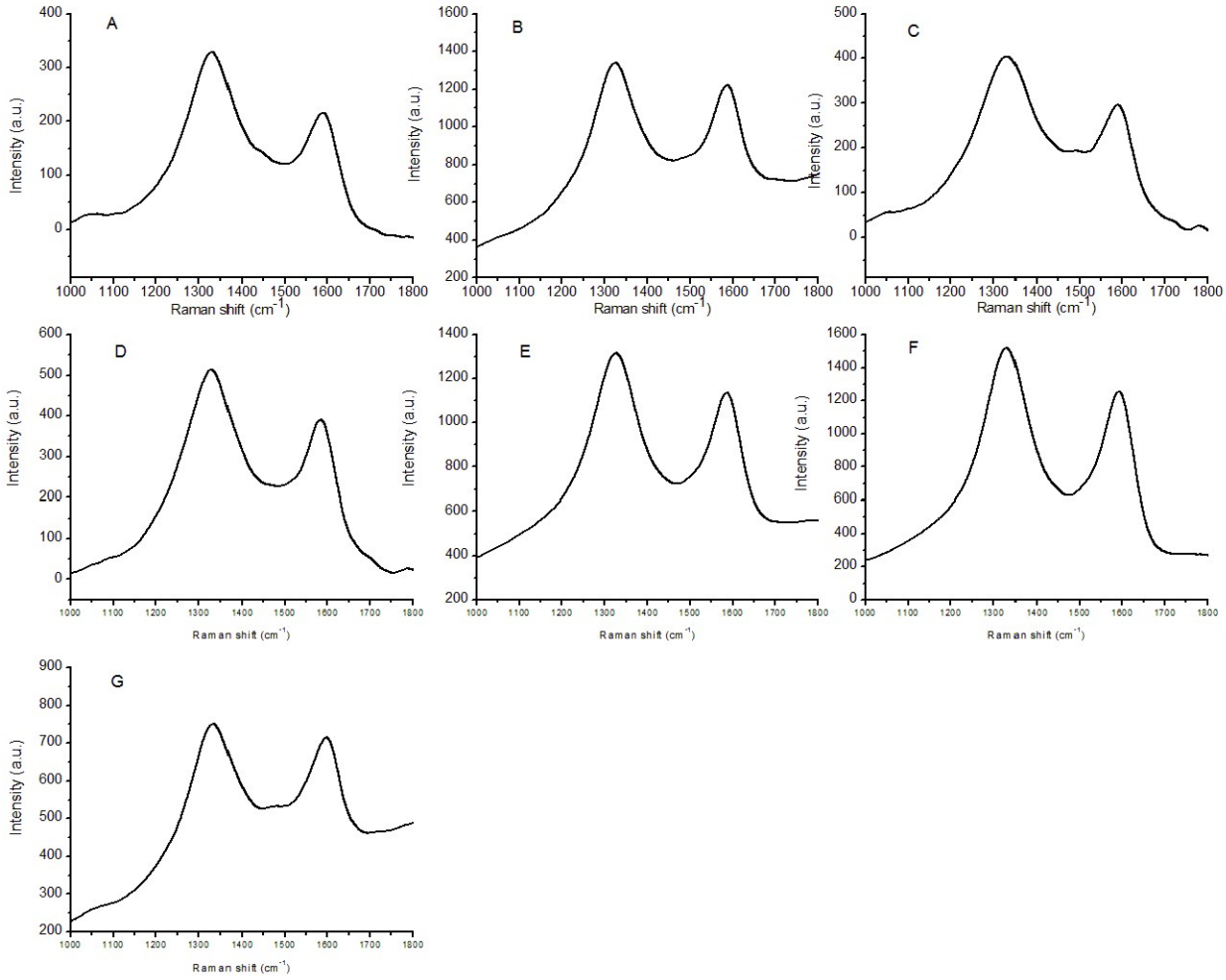

Fig. S10. Raman spectra of carbon fibers. A, KL-Raw; B, KL-L/H-Insol.; C, KL-L/H-Insol.-3.5K; D, KL-L/H-Insol.-6K; E, KL-L/H-Insol.-12K; F, 80 % KL-12K+20 % KL-Raw; G, pure PAN.

X-ray diffraction (XRD)

A Bruker D8 Discovery X-ray diffraction system (Bruker, Madison, WI) was used to analyze the graphitic structure in carbon fibers. X-ray resource was generated at 40 mA current and 40 kV voltage with Cu Ka wavelength (λ) of 1.542 Å. Diffractograms were taken in the 2θ range from 10° to 80°. Scanning step size was 0.05°, and the scanning rate was set at 1.5°/min. As shown in Fig. S11A, a crystal peak near 2θ of 21.5° was observed for all carbon fibers. This peak was assigned to (002) in a pre-graphitic turbostratic carbon.[7] The crystalline size (L_{hkl}) can be calculated from Scherrer equation: $L_{hkl} = \frac{K\lambda}{\beta \cos\theta}$ where L_{hkl} is the crystalline size, nm; K is shape factor, set as 0.94 in this calculation; λ is the X-ray wavelength (1.542 Å); β is full width at half maximum (FWHM); θ is the Bragg angle, degree. The distance between two atomic layers in crystal structure (d_{hkl}, Fig. S11B) can be calculated from the Bragg's law: $2d \sin\theta = n\lambda$, where d is distance, nm; θ is the Bragg angle, degree; n is set as 1.

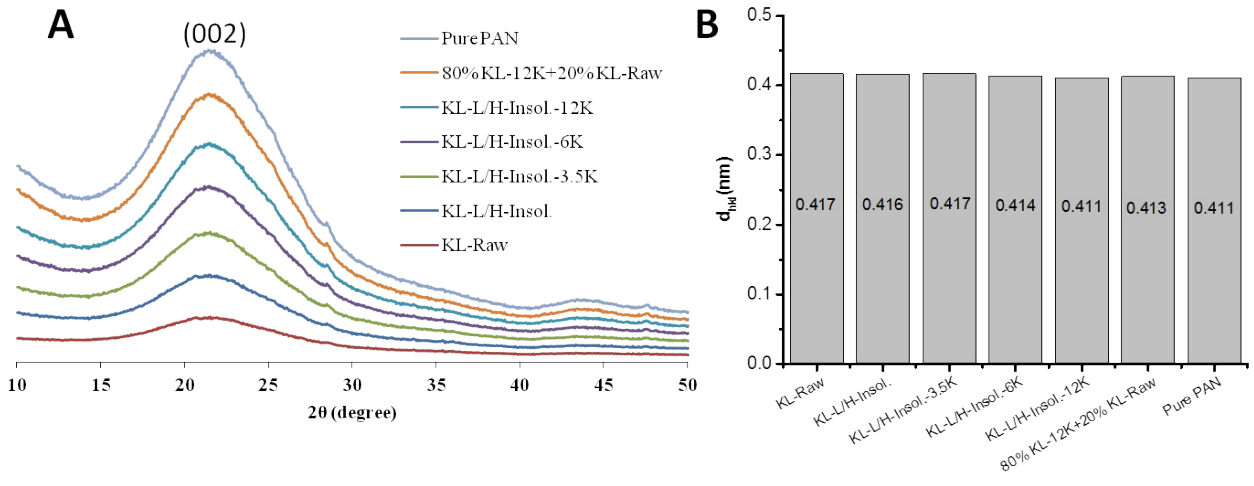

Fig. S11. XRD Diffractograms of carbon fibers (A) and the distance between two atomic layers in (002) crystalline lattices as calculated with Bragg law (B).

233 Table S3. Reduced elastic modulus of lignin-based carbon nanofiber and the commericial carbon

234 fibers as measured by nanoindentation.

Ref.	Carbon fiber	Vendor	Fiber precursor	Reduced elastic modulus (GPa)*
Fan et (2015)[9]	T700SC	Toray	PAN	23.17 ± 1.27
	K637	Mitsubishi	Pitch	10.7 ± 3.1
Maurin et al (2008)[10]	M40J	Toray	PAN	15.0 ± 4.9
	M46J	Toray	PAN	14.0 ± 4.7
Huson et al (2014)[11]	M46J	Toray	PAN	~14 GPa
Gindl-Altmutter et al (2015)[12]	Lignin micro-particles	Homemade	Kraft lignin	8.2 ± 3.04
This research	Lignin-based carbon nanofiber	Homemade	Kraft lignin/PAN (Laccase-HBT/dialysis)	21.7 ± 2.0

235 * all reduced elastic modulus data in this table were measured by nanoindentation at the transverse

236 direction of carbon fibers.

237

238

References:

1. S. Xie, Q. Sun, Y. Pu, F. Lin, X. Wang, A. Ragauskas, J. S. Yuan. *ACS Sustainable Chem. Eng.* 2017, **5**, 2215-2223.
2. C. Zhao, S. Xie, Y. Pu, R. Zhang, F. Huang, A. J. Ragauskas, J. S. Yuan. *Green Chem.* 2016, **18**, 1306-1312.
3. C.-L. Chen. *In Methods in Lignin Chemistry*; Lin, S. Y.; Dence, C. W. Eds.; Springer-Verlag: New York, 1992; pp 409–422.
4. D. S. Argyropoulos, C. Crestini. *ACS Sustainable Chem. Eng.* 2016, **4**, 5089-5089.
5. R. Maurin, P. Davies, N. Baral, C. Baley. *Appl. Comp. Mater.* 2008, **15**, 61-73.
6. W. C. Oliver, G. M. Pharr. *J. Mater. Res.* 1992, **7**, 1564-1583.
7. M. Nar, H. R. Rizvi, R. A. Dixon, F. Chen, A. Kovalcik, N. D'Souza. *Carbon* 2016, **103**, 372-383.
8. S. Kubo, J. F. Kadla. *Biomacromolecules* 2003, **4**, 561-567.
9. Z. Fan, R. Tan, K. He, M. Zhang, W. Peng, Q. Huang. *Chem. Eng. J.* 2015, **272**, 12-16.
10. R. Maurin, P. Davies, N. Baral, C. Baley. *Appl. Comp. Mater.* 2008, **15**, 61-73.
11. M. G. Huson, J. S. Church, A. A. Kafi, A. L. Woodhead, J. Khoo, J. Khoo, M.S.R.N. Kiran, J. E. Bradby, B. L. Fox. *Carbon*, 2014, **68**, 240-249.
12. W. Gindl-Altmutter, C. Fürst, A. Mahendran, M. Obersriebnig, G. Emsenhuber, M. Kluge, S. Veigel, J. Keckes, F. Liebner. *Carbon* 2015, **89,** 161-168.